Time-Variant Flexural Reliability of Posttensioned, Segmental Concrete Bridges Exposed to Corrosive Environments

Radhakrishna G. Pillai[1]; David Trejo, P.E., M.ASCE[2]; Paolo Gardoni, M.ASCE[3]; Mary Beth D. Hueste, P.E., M.ASCE[4]; and Kenneth Reinschmidt, P.E., M.ASCE[5]

Abstract: Posttensioned (PT) bridges are used on major thoroughfares because they are economical structures for traversing long spans. Special inspections of these bridges have revealed corrosion of the strands at void locations in the tendons. The integrity of these strands has significant influence on the safety of these bridges. Inspections indicate that many ducts (parts of the tendon that is supposed to protect strands from exposure to aggressive environments) are cracked and many grout holes and vents are opened, allowing direct ingress of moisture and chlorides. This paper presents a framework for assessing the flexural reliability of PT bridges exposed to various environmental conditions. The moment capacity of a PT girder is formulated using probabilistic models for the tension capacity of corroding PT strands exposed to various void and environmental conditions. Using Monte Carlo simulations, the flexural reliability of an example PT bridge is assessed. The research indicates that the flexural reliability index reaches a value below the recommended value within a relatively short period of time when moisture and chlorides infiltrate the tendons. These findings emphasize the critical need for new inspection, assessment, and repair methods for these bridge types. **DOI: 10.1061/(ASCE)ST.1943-541X.0000991.**

Author keywords: Segmental; Concrete; Bridge; Tendon; Strand; Void; Chlorides; Corrosion; Flexural; Reliability; Safety; Structural safety and reliability.

Introduction

Posttensioned (PT), segmental bridges are gaining widespread acceptance worldwide. However, the PT bridge industry has witnessed the presence of voids inside the grouted tendons and corrosion of strands leading to the failure of individual tendons and/or collapse of bridge girders. The corrosion of PT strands led to the collapse of the Bickton Meadows Footbridge and Ynys-Y-Gwas Bridge in the United Kingdom at approximately 15 and 33 years of service [Transport and Road Research Laboratory (TRRL) 1987; National Cooperative Highway Research Program (NCHRP) 1998]. Furthermore, the Niles channel, Mid-Bay, and Bob Graham Sunshine Skyway bridges in Florida experienced tendon failures [Florida Department of Transportation (FDOT) 1999, 2001a, b] at approximately 8, 13, and 16 years, respectively, after construction. The Varina-Enon Bridge in Virginia experienced tendon failure at approximately 3 years after the existing voids in the PT ducts were filled with new grout (Hansen 2007). NCHRP (1998) suggests that there is a pressing need for bridge engineers to understand the durability issues associated with PT bridges. Many state and federal highway agencies in the United States are in dire need of tools to meet this pressing need and to monitor and assess safety levels of PT bridges to plan maintenance and repair programs. Pillai et al. (2010b) developed a framework for determining the time-variant service reliability of posttensioned segmental concrete bridges exposed to corrosive environments. This paper deals with strength reliability of similar bridges.

A generalized reliability index, β, can be considered as a quantitative performance index for the safety of structural systems. In this paper, the term β is defined based on the probability that the moment demand, D_M, equals or exceeds the corresponding moment capacity, C_M. Therefore, the term β indicates a generalized flexural reliability index and is simply denoted as flexural reliability index in this paper. Based on structural reliability techniques and probabilistic models for D_M and C_M, this paper develops a framework to assess the time-variant flexural reliability index, $\beta(\mathbf{x}, t)$, of corroding PT bridges. The vector $\mathbf{x}$ indicates various parameters and random variables (i.e., the tension capacity, C_T, of strands, the void and damage conditions of tendons, environmental conditions, and the external loading, geometrical, material, and structural characteristics of the bridge) influencing D_M and C_M; and t indicates the exposure time (or the age of a PT bridge). This paper also demonstrates the application of the proposed framework by assessing the $\beta(\mathbf{x}, t)$ of a typical PT bridge.

The remaining paper is organized in the following manner. First, a review on corrosion-induced deterioration of C_M of PT bridges is provided. A general framework to determine $\beta(\mathbf{x}, t)$

[1]Assistant Professor, Building Technology and Construction Management Division, Dept. of Civil Engineering, Indian Institute of Technology Madras, Chennai, Tamilnadu 600 036, India. E-mail: pillai@iitm.ac.in

[2]Professor and Hal D. Pritchett Endowed Chair, School of Civil and Construction Engineering, Oregon State Univ., 220 Owen Hall, Corvallis, OR 97331. E-mail: david.trejo@oregonstate.edu

[3]Associate Professor, Dept. of Civil and Environmental Engineering, Univ. of Illinois at Urbana Champaign, 205 N. Mathews Ave., Urbana, IL 61801 (corresponding author). E-mail: gardoni@illinois.edu

[4]Professor, Zachry Dept. of Civil Engineering, Texas A&M Univ., 3136 TAMU, College Station, TX 77843-3136. E-mail: mhueste@civil.tamu.edu

[5]J. L. Frank/Marathon Ashland Petroleum LLC Chair in Engineering, Project Management Professor, Zachry Dept. of Civil Engineering, Texas A&M Univ., 3136 TAMU, College Station, TX 77843-3136. E-mail: kreinschmidt@civil.tamu.edu

Note. This manuscript was submitted on January 17, 2013; approved on October 29, 2013; published online on May 23, 2014. Discussion period open until October 23, 2014; separate discussions must be submitted for individual papers. This paper is part of the ***Journal of Structural Engineering***, © ASCE, ISSN 0733-9445/A4014018(10)/$25.00.

is then presented. The probabilistic models for C_M and D_M and a discussion on the random variables used in modeling C_M and D_M are then presented. Then, as an application of the developed reliability framework, the values of $\beta(\mathbf{x}, t)$ for a typical PT bridge are determined based on a set of random variables and a predefined set of parameter combinations (i.e., $\mathbf{x}$ and t). Finally, the conclusions from this study are provided. Further details on this research can be obtained from Trejo et al. (2009a) and Pillai (2009).

Corrosion-Induced Deterioration of Moment Capacity of Posttensioned Bridges

This section presents a brief overview of the typical environmental exposure and tendon conditions and corrosion mechanisms that are common in PT systems. The effect of these exposure and tendon conditions on the C_T of strands is then reviewed. Following this, the challenges associated with the estimation of the C_M of PT bridges are discussed.

Environmental Exposure and Tendon Conditions and Corrosion Mechanisms

A tendon that is placed outside the concrete and within the hollow or void space of the girder section is defined as an external tendon. A tendon that is placed inside a concrete element of the girder section is defined as an internal tendon. Fig. 1 shows the cross section at midspan of a typical PT bridge. The tendons numbered T1, T2, and T3 are external tendons. The remaining tendons are internal tendons. Further details on Fig. 1 are provided subsequently. As shown in Fig. 2, in a tendon the strands are placed inside high-density-polyethylene ducts. After posttensioning, the interstitial spaces between the duct and strands are filled with cementitious grout. The grout is designed only for corrosion protection and not for structural load bearing. Fig. 2(a) shows the cross section of a tendon with no voids. However, bleed water evaporation and poor grouting practices [American Segmental Bridge Institute (ASBI) 2000; FDOT 2001a, b; Schupack 1971, 1974, 1994, 2004] can result in the formation of voids inside these ducts, especially at the anchorage regions. These voids in conjunction with damaged tendons (cracked ducts or opened grout holes or vents) can expose the strands to water and other corrosive elements, leading to strand corrosion (TRRL 1987; NCHRP 1998; ASBI 2000; FDOT 1999, 2001a, b; Hansen 2007). Fig. 2(b) shows the cross sections of tendons with partial and full voids. Woodward (1981) reported that more than 50% of tendons in approximately 12 bridges constructed between 1958 and 1977 contained voids with sufficient size to expose the strands to aggressive conditions and accelerate corrosion. Woodward et al. (2001) found that 62% of the internal ducts contained voids that were continuous along the entire length of the tendons in a segmental PT bridge constructed in 1961. They also found that two ducts in this bridge contained no grout. More and more voids and void-induced corrosion have been detected in many PT bridges worldwide.

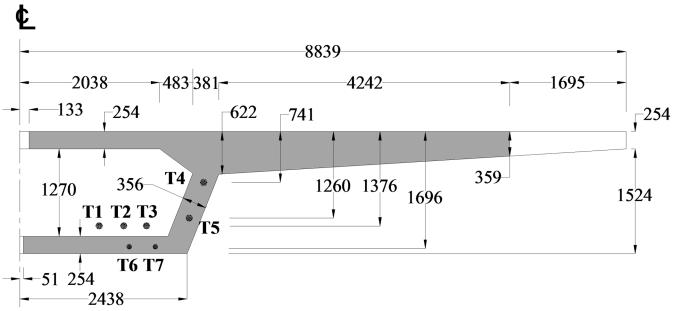

Fig. 1. Semi-cross section at midspan of a typical segmental, PT box girder (data from Trejo et al. 2009a); all dimensions are in millimeters

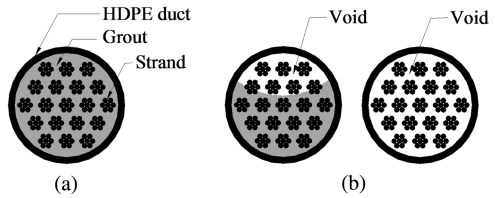

Fig. 2. Cross-sectional views of tendons with and without voids: (a) tendon with no voids; (b) tendons with partial and full voids (data from Trejo et al. 2009a)

Based on the data collected by the Texas Department of Transportation (TxDOT) (2004), it is concluded that approximately 12% of the external ducts in a PT bridge in Texas had at least one opening through which chlorides or moisture from outside can infiltrate the tendon system. Moisture and chlorides can collect inside the tendons, making direct contact with the strands and resulting in active corrosion (Woodward et al. 2001). Corrosion initiation in external tendons can occur as soon as the strands come in direct contact with the infiltrated water and/or corrosive ions. In other words, this corrosion mechanism is similar to the atmospheric corrosion, where corrosion initiates upon contact with the moisture (electrolyte) in the atmosphere. Therefore, the corrosion performance of PT bridges with external tendons cannot be assessed based on chloride diffusion through the cover concrete, which is a usual approach for predicting the corrosion performance of pretensioned bridges with internal tendons. Pillai (2009), Gardoni et al. (2009), and Trejo et al. (2009b) found that the presence of voids, moisture, and chlorides inside the tendons can significantly reduce the C_T of posttensioning strands.

Challenges in the Estimation of the Moment Capacity of Posttensioned Bridges

The tendons play a major role in the moment capacity of PT bridges. According to Poston et al. (2003), a 25% reduction in the C_T of tendons can result in a 50% or more reduction in the live load-carrying capacity of a bridge. The estimation of C_M is dependent on the estimation of the stress in the tendon and the C_T as a function of exposure conditions and time.

Ting and Nowak (1991) developed a computer algorithm to study the effect of the C_T of strands on the C_M of pretensioned beams. They assumed constant values for the initial prestress force, P_i, loss in prestress force, P_{loss}, and C_T for all the strands at the same depth in a beam. Depending on the uncertainties associated with the stress-strain and corrosion mechanisms, this might not be the case in segmental, PT bridges. Later, Cavell and Waldron (2001) developed an algorithm and studied the effect of voids in the tendons on the C_M of PT bridges. However, Cavell and Waldron (2001) did not account for the uncertainties in the C_T of individual strands.

AASHTO provide specifications for the design of segmental, PT bridges (AASHTO 1999, 2007). These specifications are calibrated to design new bridges with a target flexural reliability index, β_{target}, of 3.5 (Nowak and Collins 2000). However, not all formulations, especially the formulation for the lump sum estimate of C_M, in these design documents can be used to assess the C_M of existing segmental, PT bridges. This is because they do not account for

the possible corrosion-induced variations in the load distribution among the strands. This variation in load distribution among the strands is a result of the corrosion-induced variations in the cross-sectional areas, A_{ps}, of the individual strands. These variations in turn cause a change in the depth of the neutral axis, c. These mechanisms should be properly accounted for while estimating the C_M. In addition, the load redistribution that occurs when one or more strands fail should also be accounted for while estimating C_M. In short, the stress distribution among the corroding strands in a PT bridge is complex and dynamic. A probabilistic approach that separately considers the load in individual strands would provide more realistic estimates of the C_M of corroding segmental, PT bridges.

Modeling Time-Variant Flexural Reliability

This paper focuses on the effect of the corrosion of external tendons on the $\beta(\mathbf{x}, t)$ of existing PT bridges. Following the conventional structural reliability theory (Ditlevsen and Madsen 1996), the flexural limit state function, $g(\mathbf{x}, t)$, is defined as follows:

$$g(\mathbf{x}, t) = C_M(\mathbf{x}, t) - D_M(\mathbf{x}) \tag{1}$$

such that the event $g(\mathbf{x}, t) < 0$ represents the flexural failure. Various uncertainties are taken into account while formulating $C_M(\mathbf{x}, t)$ and $D_M(\mathbf{x})$. The uncertainties associated with the C_T and $P_{\text{loss,as-received}}$ (defined as the loss in prestressing force on an as-received strand) of individual strands, the compressive strength of concrete, f'_c, the void condition in and the damage condition of the external tendons, and the elements of applied dead load and live load are considered by defining these terms as random variables. The analytical formulation for $g(\mathbf{x}, t)$ is then programmed in *MATLAB* and incorporated into the reliability software *FERUM* (Der Kiureghian et al. 2006) to determine $\beta(\mathbf{x}, t)$. The value of P_f is calculated using Monte Carlo simulations of $g(\mathbf{x}, t)$ with a target coefficient of variation (COV) for P_f [i.e., $\text{COV}(P_f)_{\text{target}}$] of 5%. Then, β is determined as follows (Ditlevsen and Madsen 1996):

$$\beta(\mathbf{x}, t) = -\Phi^{-1}(P_f) \tag{2}$$

where Φ = cumulative distribution function of the standard normal distribution.

Moment Capacity of a Girder at Midspan

This section presents the procedures to determine the probabilistic C_M of PT bridges. These procedures use the probabilistic models for C_T developed by Pillai et al. (2010a) and Trejo et al. (2009a), the formulations for stress and strain in concrete from Todeschini et al. (1964), and the formulations for nominal tensile stress of strands from the AASHTO LRFD specifications (2007). The probabilistic models for C_T by Trejo et al. (2009a) are selected because they capture the effect of void, moisture, chloride, relative humidity (RH), and temperature (T) levels inside the tendons on the C_T of strands. The nonlinear stress-strain model for concrete by Todeschini et al. (1964) is selected because it is a single closed-form solution, and hence suitable for efficient numerical simulation. The formulation for nominal tensile stress of unbounded strands from the AASHTO LRFD specifications (2007) is used because the external tendons are unbonded and internal tendons are assumed to be unbonded.

A typical segmental box girder can be represented by an equivalent T-section. Fig. 3 shows the schematic of a typical T-section with normal stresses and forces acting on the concrete and strands at the cross section. The formulations of these compressive and tensile forces and the calculation of moment capacity are discussed next.

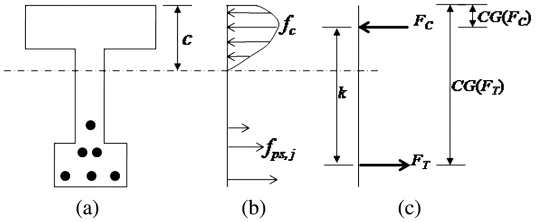

Fig. 3. Simplified cross section of a box girder showing the sectional stresses and forces (data from Trejo et al. 2009a): (a) cross section; (b) stress distribution; (c) normal forces

Compressive Forces on a Cross Section

The normal compressive stress in concrete, f_c, is calculated using the nonlinear stress-strain model developed by Todeschini et al. (1964). The maximum allowable strain at the extreme compression fiber is assumed to be 0.003, which is the maximum usable concrete compressive strain defined by the AASHTO LRFD specifications (2007). Following these, the total compressive force, F_C, on the concrete cross section and its center of gravity, $\text{CG}(F_C)$, are determined.

Tensile Forces on a Cross Section

At first, the effective prestress, f_{pe}, is calculated by subtracting the prestress losses at a given time due to long-term effects, Δf_{pLT}, from the initial prestress after anchoring, f_{pi}, as follows:

$$f_{pe,j} = f_{pi} - \Delta f_{\text{pLT},j} = \frac{0.70 \times \text{MUTS}}{A_{\text{as-received}}} - \frac{P_{\text{loss,as-received},j}}{A_{\text{as-received}}} \tag{3}$$

where the subscript j = jth strand; $P_{\text{loss,as-received},j}$ = loss in prestressing force on an as-received strand; and MUTS and $A_{\text{as-received}}$ = minimum ultimate tensile strength and cross-sectional area, respectively, of an as-received strand with negligible corrosion. Because $P_{\text{loss,as-received}}$ is a random variable, f_{pe} is a random variable. For a corroded strand, the remaining cross-sectional area, A_{ps}, is calculated as follows:

$$A_{ps,j} = C_{T,j}\left(\frac{A_{\text{as-received}}}{C_{T,\text{as-received}}}\right) \tag{4}$$

where $C_{T,\text{as-received}}$ = average tension capacity of as-received strands with negligible corrosion. The value of $C_{T,\text{as-received}}$ is typically slightly higher than its MUTS. If $A_{ps,j}$ in Eq. (4) is calculated to be zero, then the stress on the strand, $f_{ps,j}$, and $f_{pe,j}$ are set to be zero and removed from further calculations. If $A_{ps,j}$ is greater than zero, then the average stress, $f_{ps,j}$, is determined in each strand at nominal conditions using Eq. (5) for unbonded strands, provided in the AASHTO LRFD specifications (2007)

$$f_{ps,j} = \underbrace{\left[f_{pe,j} + f_{\text{empirical}}\left(\frac{d_{p,j} - c}{l_e}\right)\right]}_{f_{ps,j,\text{calculated}}} \le f_{py}; \qquad l_e = \left(\frac{2l_i}{2 + N_s}\right) \tag{5}$$

where $d_{p,j}$ = distance between the extreme compression fiber and centroid of the jth strand; l_e = effective tendon length; l_i = length of

the strand between anchorages; N_s = number of support hinges crossed by the strand between the anchorages; and f_{py} = yield strength of strand. The value of the empirical constant, $f_{\text{empirical}}$, is 6,200 and 900, when the units of stress variables (i.e., f_{pe} and f_{py}) are kN/mm^2 and ksi, respectively. The value of $f_{psj,\text{calculated}}$ varies due to the variation in c. If $f_{ps,j,\text{calculated}}$ is greater than the ultimate tensile stress capacity of strand, f_{pu}, then the strand fails in tension and is removed from further calculations by setting the corresponding $f_{ps,j}$, $f_{pe,j}P_{e,j}$, and $A_{ps,j}$ to zero. If $f_{ps,j,\text{calculated}}$ is greater than zero and less than f_{py}, then $f_{ps,j}$ is set equal to $f_{ps,j,\text{calculated}}$. If $f_{ps,j,\text{calculated}}$ is between f_{py} and f_{pu}, then $f_{ps,j}$ is set equal to f_{py} [based on the limit provided by Eq. (5)]. The tensile force, $F_{T,j}$, for each strand is then calculated by multiplying $A_{ps,j}$ with $f_{ps,j}$. Using the locations and $F_{T,j}$ values for all the strands, the total tensile force, F_T, and its center of gravity, CG(F_T) are calculated.

Moment Capacity

Once F_T and F_C are determined, the equilibrium conditions are checked prior to calculating the corresponding bending moment, M. If $(|F_T| - |F_C|)$ is greater than $0.001 \times |F_C|$, then F_T and F_C are not in equilibrium, and therefore the iterative process is repeated with another set of values for the depth of neutral axis, c, and curvature, ϕ. If $(|F_T| - |F_C|)$ is less than or equal to $0.001 \times |F_C|$, then F_T and F_C are in equilibrium and the average normal force, F, is calculated as $[(|F_T| + |F_C|)/2]$. The moment arm, k, is calculated by subtracting CG(F_C) from CG(F_T). Finally, the bending moment, M, is calculated by multiplying F and k. The entire process of calculating M is repeated with different values of ϕ and the maximum obtained value of M is defined as the C_M. To minimize computing time, the value of c and ϕ in every iterative process is determined using a smart search algorithm given in Pillai (2009). Fig. 10.3 in Pillai (2009) gives a simplified flowchart to determine moment capacity. This is reproduced in Fig. 4.

Moment Demand on the Girder at Midspan

The term D_M is modeled as a function of the external loading conditions and geometrical, material, and structural characteristics of the bridge, and not as a function of time. The dead, live, and impact loads are used in modeling D_M. The dead load due to the weight of precast box section is denoted as DL_{box}. The dead load due to the weight of the overlay, future wearing surface, and side barriers is denoted as $\text{DL}_{\text{nonbox}}$. Similarly, the unit weights of the reinforced concrete used in these elements are denoted as ρ_{box} and ρ_{nonbox}, respectively. The values of DL_{box} and $\text{DL}_{\text{nonbox}}$ are expressed as uniformly distributed loads and are calculated based on the span, cross-sectional geometry of the girder, ρ_{box} and ρ_{nonbox}. Following the procedures in AASHTO standard specifications (2002) and AASHTO LRFD specifications (2007), the design lane (LL_{lane}), truck (LL_{truck}), and tandem ($\text{LL}_{\text{tandem}}$) loads are used to calculate the total live load for HS20 and HL93 loading conditions (AASHTO 2007). In this paper, LL indicates the sum of the live and impact loads prescribed in these specifications. Using the structural mechanics principles and influence line theory, the critical section with the maximum moment is determined for the segmental girder. D_M is then defined equal to this maximum moment. The uncertainty in D_M is captured by modeling ρ_{box}, ρ_{nonbox}, LL_{lane}, LL_{truck}, and $\text{LL}_{\text{tandem}}$ as random variables.

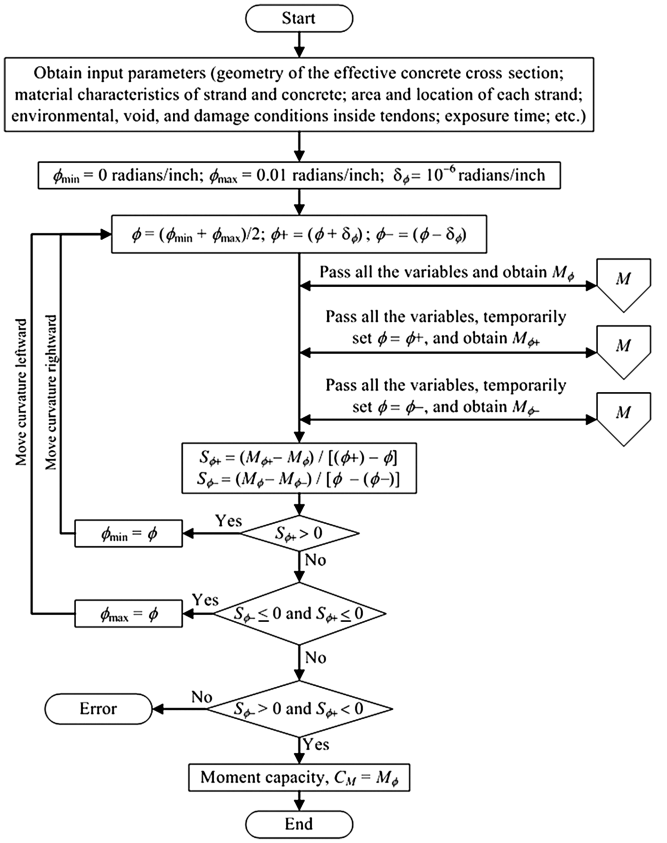

Fig. 4. Flowchart to determine moment capacity of a PT girder (reprinted from Pillai 2009)

Random Variables Influencing Flexural Reliability

The structural loading conditions, f'_c, void condition in tendon systems, damage condition of tendon systems, and C_T and P_{loss} of PT strands are the random variables that can influence the $\beta(\mathbf{x}, t)$ of PT bridges. This section presents the probabilistic modeling of these random variables (specific statistics used in the reliability analysis are presented subsequently).

Structural Load Parameters

The random variables associated with the dead load functions (i.e., DL_{box} and $\text{DL}_{\text{nonbox}}$) are the unit weight of corresponding reinforced concrete materials (i.e., ρ_{box} and ρ_{nonbox}) of the selected PT girder. Because ρ_{box} and ρ_{nonbox} are always positive, they are assumed to be independent and follow lognormal distributions. The mean estimates of ρ_{box} and ρ_{nonbox} are assumed to be equal to 2,500 kg/m^3 (155 lb/ft^3) and 2,400 kg/m^3 (150 lb/ft^3), respectively. The standard deviations are calculated based on a COV of 0.10 (Nowak and Collins 2000).

The mean values of live load parameters, LL_{lane}, LL_{truck}, and $\text{LL}_{\text{tandem}}$, are obtained using the standard procedures provided in AASHTO (2002) for HS20 loading and the AASHTO LRFD specifications (2007) for HL93 loading conditions. In addition, the AASHTO LRFD specifications (2007) provide multiple lane factors equal to 1.20, 1.00, 0.85, and 0.65 for one, two, three, and greater than three lanes, respectively. Per Nowak and Collins (2000), live loads are modeled as normal distributions with a bias factor and COV of 1.25 and 0.18 for the joint effect of live and impact loading.

Compressive Strength of Concrete

In general, contractors provide concrete with an actual compressive strength, f'_c, higher than the specified compressive strength, $f'_{c,\text{specified}}$, and there exists an uncertainty in the value of f'_c. Because f'_c is a positive number, it is expressed as a lognormal distribution. The COV of f'_c is assumed to be 0.15 (Nowak and Collins 2000).

Void and Damage or Opening Conditions

The void and damage conditions are defined on the basis of the probability of the presence of a voided tendon (P_{VT}) and a damaged tendon (P_{DT}), respectively. A voided tendon is defined as a tendon with at least one void. A damaged tendon is defined as a tendon with at least one unsealed hole or vent at the anchorage region or an unsealed vent or crack on the PT ducts. As Woodward (1981) and Woodward et al. (2001) determined, P_{VT} can be determined based on inspection of sample bridges or tendons or assumed based on sound engineering judgment. Similarly, P_{DT} can be determined or assumed. The two void conditions considered are no void and void conditions. The two damage conditions considered are no damage and damaged conditions. Therefore, the void and damage conditions are modeled as binomial distributions using P_{VT} and P_{DT} as model parameters (i.e., success probabilities). Based on the data from TxDOT (2004), P_{VT} and P_{DT} are calculated to be 78.6 and 12%, respectively.

Tension Capacity of Strands

Trejo et al. (2009a) and Pillai et al. (2010a) developed probabilistic models to predict the C_T of strands subjected to various void and environmental conditions. The environmental conditions included T, RH, and chloride concentration in the grout and infiltrated solution ($\%g\text{Cl}^-$ and $\%s\text{Cl}^-$, respectively). Among these, the following four models are used to assess $\beta(\mathbf{x}, t)$ of segmental, PT bridges (Trejo et al. 2009a; Pillai et al. 2010a):

$$\text{Model1: } C_T \sim \text{MUTS} \times \text{lognormal}(1.011, 0.0049) \tag{6}$$

$$\text{Model2: } C_T = \text{MUTS} \times [A(h_{t_{\text{CA}}})^{n_{\text{CA}}} + \sigma\varepsilon] \tag{7}$$

$$\text{where, } A = \theta_1\{\theta_2 - \theta_3 \exp(h_{\text{RH}}) - \theta_4 \exp[h_{\%g\text{Cl}^-} \exp(h_{\text{RH}})h_T]\}^{\theta_5}$$

$$\text{Model3: } C_T = \text{MUTS} \times [\theta_1(\theta_2 - \theta_3 h_{\%s\text{Cl}^-} h_{t_{\text{WD}}})^{\theta_4} + \sigma\varepsilon] \tag{8}$$

$$\text{Model4: } C_T = \text{MUTS} \times \{\theta_1[\theta_2 - \theta_3 h_{t_{\text{WD}}} - \theta_4 \ln(h_{\%s\text{Cl}^-})h_{t_{\text{WD}}}]^{\theta_5} + \sigma\varepsilon\} \tag{9}$$

The Notation and Table 1 show the definitions of the explanatory functions or predictor variables (i.e., $h_{\text{RH}}, h_T, h_{\%s\text{Cl}^-}, h_{\%g\text{Cl}^-}$, $h_{t_{\text{WD}}}, h_{t_{\text{CA}}}$) and the statistics of the unknown model parameters (i.e., θ_i and σ). Trejo et al. (2009a) provides further details on the correlation coefficients between the estimated model parameters. An appropriate probabilistic model for C_T of each strand is selected based on the tendon type (i.e., external or internal tendon), the predefined environmental condition, and the randomly obtained void and damage conditions. Fig. 5 shows the method used to select the strand capacity models; the circles indicate the model number for each exposure category (i.e., combinations of tendon type, environmental, void, and damage conditions). The environmental condition can be manually selected per the user's choice. The void and damage conditions are randomly obtained as discussed previously (Table 2). Because the wet-dry condition in a tendon will occur only if there is damage to the tendon system, the no damage condition corresponding to the wet-dry conditions is not shown in Fig. 5.

Table 1. Mean Estimates of Model Parameters in the Strand Capacity Models

Model parameters	Model 2	Model 3	Model 4
θ_1	7.7492 (0.9532)	0.9983 (0.0014)	0.9463 (0.0064)
θ_2	0.1637 (0.0018)	1.0105 (0.0022)	1.0333 (0.0056)
θ_3	0.0030 (0.0008)	1.6785 (0.1362)	0.3567 (0.0648)
θ_4	0.0002 (0.0000)	1.3576 (0.0648)	0.0285 (0.0015)
θ_5	1.0924 (0.0617)	—	2.0301 (0.0773)
σ	0.0619 (0.0047)	0.0117 (0.0011)	0.0350 (0.0107)

Note: Values in parenthesis indicate standard deviations.

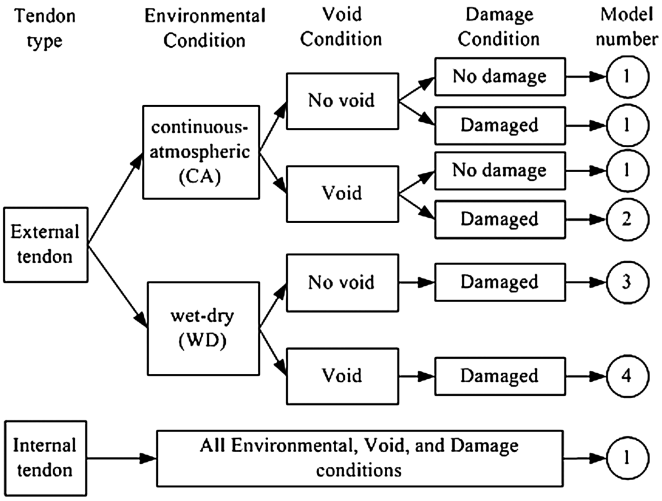

Fig. 5. Method to select the strand capacity models (data from Trejo et al. 2009a)

Table 2. Random Variables Used for the Reliability Assessment of Example PT Bridge

Random variables	Distribution (mean, standard deviation)
Void condition	~Binomial(0.79, 0.407)
Damage condition	~Binomial(0.12, 0.325)
Error term in the strand capacity model, ε	~Normal(0, 1)
Prestress loss of as-received strand, $P_{\text{loss,as-received}}$	~Lognormal(18,300,2,700) kN ~Lognormal(4,123,618) kips
Compressive strength of concrete, f'_c	~Lognormal(41.3, 6.2) MPa ~Lognormal(6, 0.9) ksi
Unit weight of concrete in the box girder, ρ_{box}	~Lognormal(2,500,250)kg/m^3 ~Lognormal(155, 15.5) lbs/ft^3
Unit weight of concrete inoverlay, future wearing surface, and side barriers, ρ_{nonbox}	~Lognormal(2,400,240) kg/m^3 ~Lognormal(150, 15.0) lbs/ft^3
Live load due to multiple lane load, LL_{lane}	~Normal(7.3, 1.5) kN/m ~Normal(0.5, 0.1) kip/ft
Live load due to design truck load, LL_{truck}	~Normal(1,115, 20) kN ~Normal(25.6, 4.6) kips
Live load due to design tandem load, $\text{LL}_{\text{tandem}}$	~Normal(89, 16) kN ~Normal(20.0, 3.6) kips

One additional point to be discussed is that of the insignificance of corrosion as a spatial issue in this analysis of posttensioned systems. In a pretensioned beam, the development length of the strand embedded in concrete influences the capacity. This paper addresses externally, posttensioned, grouted bridges. In such posttensioned bridges, if a strand fails at any point along its entire length, that strand will have no contribution to the girder capacity. Therefore, the spatial issue of corrosion of strands was not considered.

Prestress Loss of Strands

The prestress loss in the strands can be estimated using the AASHTO lump sum estimate, which is intended to quantify long-term losses for two reasons. At first, the long-term losses due to creep and shrinkage plateau over time and the lump sum estimate will not change significantly for the time points considered in this study. Second, the stress in the strands at ultimate conditions will go significantly beyond the effective prestress and the results are less sensitive to the long-term loss estimates as compared with reliability assessment of the girders at service conditions. The use of a time-variant solution for prestress losses would add significant computational effort to this analysis. Considering all these, this paper followed the AASHTO LRFD lump sum estimation method and modeled (using lognormal distribution) the $P_{\text{loss,as-received}}$ as follows:

$$P_{\text{loss,as-received}} \sim A_{\text{as-received}} \times \text{lognormal}[\overline{\Delta f}_{p\text{LT}}, \overline{\Delta f}_{p\text{LT}} \times \text{COV}(\Delta f_{p\text{LT}})] \quad (10)$$

where $\overline{\Delta f}_{p\text{LT}}$ and $\text{COV}(\Delta f_{p\text{LT}})$ = mean and COV of $\Delta f_{p\text{LT}}$. The value of $A_{\text{as-received}}$ for a 15-mm (0.6-in.) diameter PT strand is 140 mm^2 (0.217 in.^{2}). The value of $\overline{\Delta f}_{p\text{LT}}$ is assumed to be 131 MPa (19,000 psi), which is the AASHTO LRFD (2007) specified lump sum estimate of $\overline{\Delta f}_{p\text{LT}}$ in box girders, and the $\text{COV}(\Delta f_{p\text{LT}})$ is assumed to be 0.15. In this way, the mean and standard deviation of $P_{\text{loss,as-received}}$ are calculated to be 18 kN (4,123 lbs) and 2.8 kN (618 lbs), respectively.

Assessing Flexural Reliability of a Typical Posttensioned Bridge

This section first defines the typical segmental, PT bridge, and parameter combinations (representing loading and exposure conditions) for the flexural reliability analysis. Then the results on $\beta(\mathbf{x}, t)$ for the typical PT bridge subjected to various loading and exposure conditions are presented.

Definition of a Typical PT Bridge and Parameter Combinations

Fig. 1 shows one-half of the symmetrical cross section of a typical PT girder. The shaded region indicates one-half of the effective cross section, per AASHTO LRFD specifications (2007), used to estimate the flexural limit state function, $g(\mathbf{x}, t)$, as defined in Eq. (1). Fig. 1 also shows the locations of eight internal and six external tendons at midspan. The tendons T1 through T5 contain 19 strands each and T6 and T7 contain 12 strands each. All the strands are 15 mm (0.6 in.) in nominal diameter and meet the ASTM A416 (2002) specifications. For the calculation of D_M, the PT girder is assumed to be simply supported with a clear span of 30.5 m (100 ft). Fig. 6 shows the parameter combinations considered for the reliability assessment of the example PT bridge.

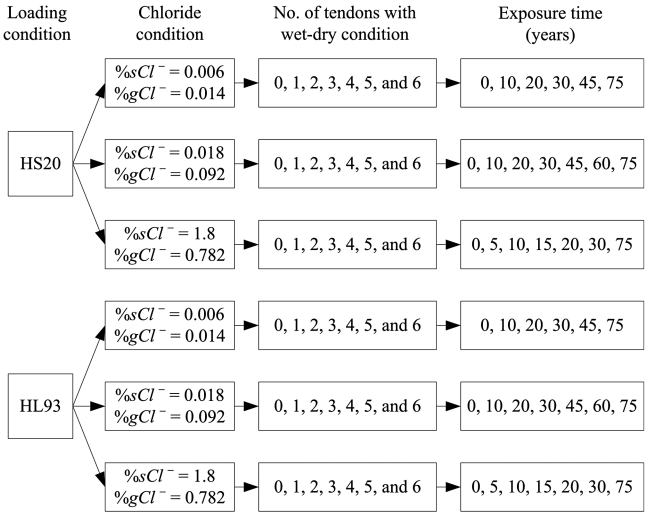

Other parameters: Ambient RH = 70%, RH inside undamaged tendons = 50%, T = 70°F (24.4 °C), ϕ_{wet} = 2/12 = 0.17, n_{CA} = − 0.005

Fig. 6. Combinations of parameters for the reliability assessment program

The loading condition indicates that HS20 and HL93 loading conditions are considered. The chloride condition indicates that three chloride conditions (each condition is defined based on $\%s\text{Cl}^-$ and $\%g\text{Cl}^-$ levels) are considered. Based on cyclic polarization tests, Trejo et al. (2009a) concluded that the critical chloride threshold level for PT strands is above $0.06\%s\text{Cl}^-$. Therefore, two levels below the critical chloride threshold (i.e., 0.006 and $0.018\%s\text{Cl}^-$) and one level above the critical chloride threshold ($1.8\%s\text{Cl}^-$) were selected for the reliability assessment. As shown in the number of tendons with wet-dry condition, the effects of wet-dry conditions with 0.006, 0.018, and $1.8\%s\text{Cl}^-$ levels in 0, 1, 2, 3, 4, 5, and 6 external tendons on $\beta(\mathbf{x}, t)$ are assessed. The tendons without wet-dry conditions will be assumed to have a continuous-atmospheric exposure condition with 0.014, 0.092, or $0.782\%g\text{Cl}^-$ level. The age of the bridge or exposure time, t, at which $\beta(\mathbf{x}, t)$ will be determined are provided in the exposure time in Fig. 6. The exposure times are selected such that a better estimation of intermediate values of $\beta(\mathbf{x}, t)$ can be obtained, especially when $\beta(\mathbf{x}, t)$ changes rapidly as a function of t. When exposed to 0.006, 0.018, and $1.8\%s\text{Cl}^-$ conditions (with ϕ_{wet} equal to 0.17, which corresponds to 2 months of wet time and 10 months of dry time in every year), the time required for the complete corrosion of strands (i.e., cross-sectional area becomes zero) are 57, 45, and 23 years, respectively. For all the cases, five values of t that are less than or equal to the time required for the complete corrosion of strands were considered. Table 2 summarizes the definitions of all the random variables used for the assessment of reliability of the example PT bridge.

Table 2 shows that the variables account for total mean DL and LL of 510 and 61 kips (2270 and 271 kN), respectively, for the 30.5-m span considered in the example bridge. In other words, DL and LL account for 89 and 11%, respectively, of the total load. This clearly indicates that the effect of LL is significantly lower than that of DL. DL can be considered as a time-invariant parameter, whereas LL can be time-variant. Moreover, the time-variant changes in LL can vary significantly as the bridge span, geographic location, human behavior, and government regulations

change. Also, the effect of this potential variation in LL can be further reduced due to these factors. Most importantly, reliable information on the time-variant changes in LL for various geographic locations is not available. Therefore, the authors took the representative standard LL given in the AASHTO *LRFD Bridge Design Specifications* (1998) and considered D_M as a random variable, which is calculated using the DL (based on the bridge geometry) and LL [based on HS-20 and HL-93 loading given in the AASHTO LRFD specifications (2007)] and statistical characteristics provided in Nowak and Collins (2000).

Time-Variant Flexural Reliability Index

This section presents the values of $\beta(\mathbf{x}, t)$ and P_f of the selected PT bridge assessed using the developed flexural reliability framework and based on $\text{COV}(P_f)_{\text{target}} = 0.05$. The designation 13822, "Bases for Design of StructuresAssessment of Existing Structures" of International Organization of Standardization (ISO 2001), suggests β_{target} values of 2.3, 3.1, 3.8, and 4.3 (corresponding to P_f of 1.0×10^{-2}, 9.7×10^{-4}, 7.2×10^{-5}, and 8.5×10^{-6}) for structures with very low, low, medium, and high consequences of failure, respectively. The consequence of failure of large amounts of structures in a city due to an earthquake could be considered as medium or high (depending on the magnitude of damage). The consequence of failure of a nuclear power plant could also be considered medium or high (depending on the toxicity of radiation and the proximity to a human populated area). In comparison with these cases, the consequence of failure of a typical segmental, PT bridge could be considered as low or medium, especially for segmental, PT bridges on major urban highways. The following discussions include comparisons of the estimated reliability with the β_{target} used in the calibration of the AASHTO LRFD specifications (2007) (i.e., 3.5) and recommended by ISO (2001) for flexural failure with low consequences of failure (i.e., 3.1).

Flexural Reliability When Strands are in As-Received Condition

For the selected PT bridge, $\beta(\mathbf{x}, t)$ remains above 3.5 (corresponding to a probability of flexural failure, P_f, equal to 2.3×10^{-4}) when all the strands are in as-received condition (i.e., when $t = 0$). However, the actual value of $\beta(\mathbf{x}, t)$ for this case could not be determined because the number of failure cases after 50 million Monte Carlo simulations was 0 and the simulation process was ended before attaining $\text{COV}(P_f)_{\text{target}}$. In addition, no flexural failure was observed among 50 million simulations when either the HL93 or HS20 loading were applied and only one tendon (constituting approximately 8% of total tendons) failed. Figs. 7(a–c) show the variation of $\beta(\mathbf{x}, t)$ with time when exposed to 0.006, 0.018, and 1.8%$s\text{Cl}^-$ solutions, respectively. In these figures, the horizontal lines with long dashes indicate the basis (i.e., $\beta_{\text{target}} = 3.5$) for the calibration of the AASHTO LRFD specifications (2007) document for ultimate conditions. The horizontal lines with short dashes indicate the β_{target} (i.e., 3.1) for a failure case with low consequences of failure [per ISO (2001)] and this corresponds to a P_f of 9.7×10^{-4}. The dashed and solid curves indicate the cases with HS20 and HL93 loading conditions, respectively. The hollow and solid data markers also indicate the cases with HS20 and HL93 loading conditions, respectively. Different data markers are used to represent the number of tendons subjected to wet-dry exposure cycles (i.e., denoted as WDT in Fig. 7).

Flexural Reliability When Strands are Exposed to Chloride Solutions

Fig. 7(a) shows the variation of $\beta(\mathbf{x}, t)$ with time when exposed to 0.006%$s\text{Cl}^-$ solution. Most of the $\beta(\mathbf{x}, t)$ values that are above 3.5 could not be obtained due to the significant computing requirement and time; the corresponding curves or data markers are not shown in Fig. 7(a). When only two tendons are subjected to HS20 loading and exposed to 0.006%$s\text{Cl}^-$ solution (hollow square markers), the value of $\beta(\mathbf{x}, t)$ at 75 years is more than 3.5. For this case, when subjected to HL93 loading (solid square markers), the $\beta(\mathbf{x}, t)$ drops below 3.5 in approximately 30 years and stays above 3.1 up to 75 years. When more than two tendons are exposed to wet-dry cycles (all triangular markers), the maximum time needed for $\beta(\mathbf{x}, t)$ to drop below 3.5 is 25 years and to drop below 3.1 is 36 years. In the most severe case with HL93 loading and six tendons with wet-dry exposure, it takes only approximately 15 years for $\beta(\mathbf{x}, t)$ to drop below 3.1. Figs. 7(b and c) show the variations in $\beta(\mathbf{x}, t)$ with time when exposed to 0.018 and 1.8%$s\text{Cl}^-$ solutions, respectively. In general, the time estimates are less than the time estimates when exposed to 0.006%$s\text{Cl}^-$ solution. Table 3 summarizes the major time estimates from Figs. 7(a–c).

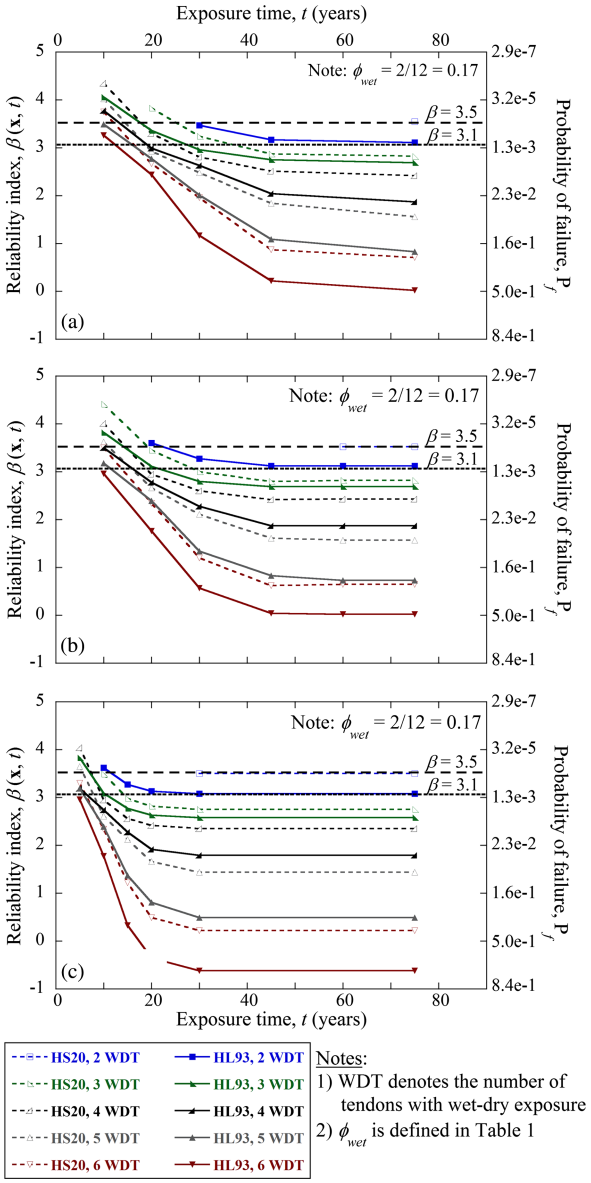

Fig. 7. Time-variant flexural reliability of the typical PT bridge: (a) 0.006%$s\text{Cl}^-$; (b) 0.018%$s\text{Cl}^-$; (c) 1.8%$s\text{Cl}^-$

Table 3. Approximate Time in Years Required for $\beta(x,t)$ to Reach Recommended β_{target}

Loading condition	%sCl^-	Number of external tendons with wet-dry conditions							
		1		2		3		6	
		Recommended values of β_{target}							
		3.5	3.1	3.5	3.1	3.5	3.1	3.5	3.1
HS20	0.006	>75	>75	>75	>75	25	36	12	16
	0.018	>75	>75	>75	>75	18	28	10	13
	1.8	>75	>75	>75	>75	10	14	<5	11
HL93	0.006	>75	>75	30	>75	17	27	<10	12
	0.018	>75	>75	22	>75	14	21	<10	<10
	1.8	>75	>75	11	>75	7	10	<5	<5

The framework developed in this research can assist bridge owners and managers in developing an efficient bridge management tool that will improve the safety and economy of these structures. As reported, aggressive environmental exposure conditions can lead to strand corrosion and failure: this has been observed in the PT bridges in Florida and Virginia. The results presented in this paper clearly show that the flexural reliability of segmental, PT bridges with voids in the tendons exposed to moisture and/or chlorides is significantly reduced within a relatively short time period. To prevent reduction in the flexural reliability of these bridges, tendons must be kept free of moisture and chlorides. Effective inspection, assessment, and repair methods should be developed to economically maintain high levels of safety for these bridges.

Conclusions

This paper developed an analytical framework to predict the flexural reliability index, $\beta(\mathbf{x},t)$, of posttensioned, segmental concrete bridges subjected to various structural and environmental loading conditions. The reliability framework is formulated based on the probabilistic moment demand and capacity models. The probabilistic model for the moment demand was developed using the AASHTO HS20 and HL93 load conditions. The time-variant moment capacity was modelled as a function of void, damage, and environmental conditions associated with the tendons and the structural, geometrical, and material characteristics of the cross section at midspan. The major contributions of the developed reliability framework are that they account for the effects due to (1) the corrosion-induced variations in the cross-sectional areas and associated load distribution among the strands, (2) the redistribution of stresses upon failure of one or more strands, and (3) the uncertainties in the tension capacity and prestress loss, void and damage conditions of tendons, the compressive strength and unit weight of concrete, and live load conditions. It is concluded that $\beta(\mathbf{x},t)$ can be estimated and used as a long-term safety indicator of PT bridges.

A typical PT bridge was defined to demonstrate the application of the developed reliability model. For this typical PT bridge, the following conclusions are drawn based on the predefined set of parameters. When all the strands are in the as-received conditions, $\beta(\mathbf{x},t)$ is above the β_{target} used for calibrating the AASHTO LRFD specifications (2007) (i.e., 3.5) and recommended by ISO 13822 (2001) for the cases with low consequences of failure (i.e., 3.1). If one tendon is exposed to wet-dry cycles and fails in tension due to high stress levels, the value of $\beta(\mathbf{x},t)$ stays above 3.5. If two tendons are exposed to wet-dry cycles and fail in tension due to high stress levels, the value of $\beta(\mathbf{x},t)$ drops below 3.5 but stays above 3.1. Furthermore, when the bridge is subjected to HS20 loading and three or more external tendons are exposed to wet-dry cycles with 0.006% chloride solution, the value of $\beta(\mathbf{x},t)$ drops below 3.5 within 25 years and below 3.1 within 35 years. These time estimates reduce to approximately 10 and 13 years when exposed to wet-dry cycles with 1.8% chloride solution.

The results demonstrate that these calculations, although computationally intensive, can readily be performed with current technology. The current research clearly shows the importance of preventing the ingress of water and chlorides into the tendons of segmental, PT bridges. Effective and frequent inspection, assessment, and repair methods are needed to maintain high levels of safety for these bridge types.

The authors recommend additional research in the following areas: (1) the development of probabilistic models for corrosion-induced loss in the tension capacity of strands in internal tendons; (2) the development of a framework for considering continuous support conditions and a combination of simply supported conditions (for dead loads and select tendons) and continuous support conditions (for live load and select tendons), depending on the bridge construction and erection sequence; (3) the development of models that consider multiaxial bending, shear, and torsion mechanisms; and (4) the development of probabilistic models to account for the long-term effects of prestress losses due to creep and shrinkage effects.

Acknowledgments

This research was performed at Texas Transportation Institute and Zachry Department of Civil Engineering, Texas A&M University, College Station, Texas, through a sponsored project from the Texas Department of Transportation (TxDOT), Austin, Texas. This support is much appreciated. Support from project directors Jaime Sanchez, Maxine Jacoby, Dr. German Claros, and Brian Merrill; program coordinator Keith Ramsey; Dean Van Landuyt; Kenneth Ozuna; Steve Strmiska; Tom Rummel; and other TxDOT engineers is acknowledged. The authors also acknowledge the assistance from Dr. Daren Cline, Ramesh Kumar, and Byoung Chan Jung during this research.

Notation

The following symbols are used in this paper:

$A_{\text{as-received}}$ = cross-sectional area of as-received strand;
B = reliability index;
C_M = moment capacity;
C_T = tension capacity;
$C_{T,\text{as-received}}$ = tension capacity of as-received strand;
c = depth of neutral axis at midspan of the girder;
D_M = moment demand;
DL_{box} = dead load due to precast concrete box section;
$\text{DL}_{\text{nonbox}}$ = dead load due to concrete overlay, wearing surface, and side barriers;
E_c = elastic modulus of concrete;
F = normal force in concrete;
F_C = normal compressive force;
F_T = normal tensile force;
f_c = normal compressive stress in concrete;
f'_c = actual compressive strength of concrete;
$f'_{c,\text{specified}}$ = specified compressive strength of concrete;
f_{pe} = effective prestress in strand;

f_{pi} = initial prestress after anchoring;
f_{ps} = total stress in prestressing strand;
f_{pu} = ultimate tensile strength of strand;
f_{py} = yield strength of prestressing strand;
$g(\mathbf{x}, t)$ = flexural limit state function;
h_{RH} = ambient relative humidity (%)/ maximum relative humidity (%) = RH(%)/100;
h_T = ambient exposure temperature (°F) = T (°F);
$h_{t_{CA}}$ = total at mospheric exposure time (years)/ standardizing factor = $t_{CA}/0.75$;
$h_{t_{WD}}$ = $\phi_{wet} \times$ total exposure time (years) = $\phi_{wet} \times t_{WD}$;
$h_{\%gCl^-}$ = %Cl^-in the grout (by weight)/ $\%sCl^-_{saturatedchloridesolution} = \%gCl^-/35.7$;
$h_{\%sCl^-}$ = %Cl^- in the water inside the tendon/ $\%\ sCl^-_{saturatedchloridesolution} = \%sCl^-/35.7$;
j = jth strand;
k = moment arm;
LL_{lane} = live load based on lane load;
LL_{tandem} = live load based on tandem load;
LL_{truck} = live load based on truck load;
l_e = effective tendon length (inches);
l_i = length of the strand between anchorages (inches);
M = bending moment;
N = number of support hinges crossed by the strand between the anchorages;
n_{CA} = constant based on field information = −0.005;
P_f = probability of flexural failure;
$P_{f,target}$ = target probability of flexural failure;
$P_{loss,as\text{-}received}$ = prestress loss in as-received strands;
T = temperature;
t = exposure time or age of bridge;
WDT = number of tendons with wet-dry exposure;
$\mathbf{x}$ = vector of influential parameters and variables;
β_{target} = target reliability index;
$\beta(\mathbf{x}, t)$ = time-variant reliability index;
Δf_{pLT} = prestress loss due to long term effects;
ε = standard normal random variable, ~N(0, 1);
θ_i = unknown model parameter;
ρ_{box} = unit weight of concrete in the box section;
ρ_{nonbox} = unit weight of concrete in the overlay, wearing surface, and side barriers;
σ = standard deviation of model error;
Φ = cumulative distribution function of the standard normal distribution;
ϕ = curvature at midspan of the girder; and
ϕ_{wet} = wet time (in months) in a year divided by 12.

References

AASHTO. (1998). *LRFD bridge design specifications*, 2nd Ed., Washington, DC.

AASHTO. (1999). *Guide specifications for design and construction of segmental concrete bridges*, 2nd Ed., Washington, DC.

AASHTO. (2002). *Standard specifications for highway bridges*, 17th Ed., Washington, DC.

AASHTO. (2007). *LRFD bridge design specifications*, 4th Ed., Washington, DC.

American Segmental Bridge Institute (ASBI). (2000). *American segmental bridge institute grouting committee: Interim statement on grouting practices*, Phoenix.

ASTM. (2002). "Standard specification for steel strand, uncoated-wire for prestressed concrete." *A416*, West Conshohoken, PA.

Cavell, D. G., and Waldron, P. (2001). "Parametric study of the residual strength of deteriorating simply-supported post-tensioned concrete bridges." *Struct. Build.*, 146(4), 341–352.

Der Kiureghian, A., Haukaas, T., and Fujimura, A. (2006). "Structural reliability software at the University of California, Berkeley." *Struct. Saf.*, 28(1–2), 44–67.

Ditlevsen, O., and Madsen, O. H. (1996). *Structural reliability methods*, Wiley, Chichester, U.K.

Florida Dept. of Transportation (FDOT). (1999). *Corrosion evaluation of post-tensioned tendons on the Niles Channel Bridge*, Tallahassee, FL.

Florida Dept. of Transportation (FDOT). (2001a). *Mid-bay bridge post-tensioning evaluation—final report*, Corven Engineering, Tallahassee, FL.

Florida Dept. of Transportation (FDOT). (2001b). *Sunshine skyway bridge post-tensioned tendons investigation*, Parsons Brinckerhoff Quade and Douglas, Tallahassee, FL.

Gardoni, P., Pillai, R. G., Trejo, D., Hueste, M. D., and Reinschmidt, K. (2009). "Probabilistic capacity models for corroding posttensioning strands calibrated using laboratory results." *J. Eng. Mech.*, 10.1061/(ASCE)EM.1943-7889.0000021, 906–916.

Hansen, B. (2007). "Forensic engineering: Tendon failure raises questions about grout in post-tensioned bridges." *Civ. Eng. News*, 17–18.

International Organization for Standardization (ISO). (2001). *Bases for design of structures—Assessment of existing structures 13822*, Geneva, Switzerland.

National Cooperative Highway Research Program (NCHRP). (1998). "Durability of precast segmental bridges." *NCHRP Web Document No.15, Project 20-7/Task 92*, Transportation Research Board, National Research Council, Washington, DC.

Nowak, A. S., and Collins, K. R. (2000). *Reliability of structures*, McGraw-Hill, Boston.

Pillai, R. G. (2009). "Electrochemical characterization and time-variant structural reliability assessment of post-tensioned, segmental concrete bridges." Ph.D. dissertation, Zachry Dept. of Civil Engineering, Texas A&M Univ., College Station, TX.

Pillai, R. G., Gardoni, P., Trejo, D., Hueste, M. D., and Reinschmidt, K. F. (2010a). "Probabilistic models for the tensile strength of corroding strands in posttensioned, segmental concrete bridges." *J. Mater. Civ. Eng.*, 10.1061/(ASCE)MT.1943-5533.0000096, 967–977.

Pillai, R. G., Hueste, M. D., Gardoni, P., Trejo, D., and Reinschmidt, K. F. (2010b). "Time-variant service reliability of post-tensioned, segmental, concrete bridges exposed to corrosive environments." *Eng. Struct.*, 32(9), 2596–2605.

Poston, W. R., Frank, K. H., and West, J. S. (2003). "Enduring strength." *Civ. Eng.*, 73(9), 58–63.

Schupack, M. (1971). "Grouting tests on large PP tendons for secondary nuclear containment structures." *PCI J.*, 16(2), 85–97.

Schupack, M. (1974). "Admixture for controlling bleed in cement grout used in post-tensioning." *PCI J.*, 16(2), 28–39.

Schupack, M. (1994). "Durability study of a 35-year-old post-tensioned bridge." *Concr. Int.*, 16(2), 54–58.

Schupack, M. (2004). "PT grout: Bleedwater voids." *Concr. Int.*, 26(8), 69–77.

Texas Dept. of Transportation (TxDOT). (2004). "Critical evaluation and condition assessment of post-tensioned bridges in Texas—Final Report." Austin, TX.

Ting, S.-C., and Nowak, A. S. (1991). "Effect of tendon-area loss on flexural behavior of P/C beams." *J. Struct. Eng.*, 10.1061/(ASCE)0733-9445(1991)117:4(1127), 1127–1143.

Todeschini, C. E., Bianchini, A. C., and Kesler, C. E. (1964). "Behaviour of concrete columns reinforced with high strength steels." *ACI J.*, 61(67), 701–716.

Transport and Road Research Laboratory (TRRL). (1987). "Seventh report of the committee for the two years ending July 1987." *EA/88/4*, Standing Committee on Structural Safety, Crowthorne, U.K.

Trejo, D., et al. (2009a). "Effects of voids in grouted, post-tensioned, concrete bridge construction." *Rep. No. 0-4588-1*, Texas Transportation Institute, Texas Dept. of Transportation, Austin, TX.

Trejo, D., Pillai, R. G., Hueste, M. D., Reinschmidt, K. F., and Gardoni, P. (2009b). "Parameters influencing corrosion and tension capacity of post-tensioning strands." *ACI Mater. J.*, 106(2), 144–153.

Woodward, R., Cullington, D., and Lane, J. (2001). "Strategies for the management of post-tensioned concrete bridges." *Current and future trends in bridge design, construction, and maintenance 2: Safety, economy, sustainability, and aesthetics*, Thomas Telford, Hong Kong, 23–32.

Woodward, R. J. (1981). "Conditions within ducts in post-tensioned prestressed concrete bridges." *LR 980*, Transport and Road Research Laboratory, Dept. of Transport, Crowthorne, Berkshire, U.K.